

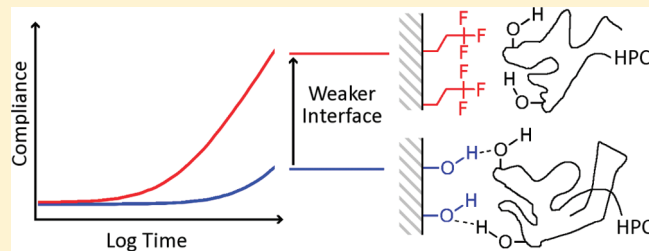
# Time-Dependent Relaxations in Thin Hydroxypropyl Cellulose Coatings: The Role of Buried Interfaces

Peter M. Johnson, John A. Howarter, and Christopher M. Stafford\*

Polymers Division, National Institute of Standards and Technology, 100 Bureau Drive, Gaithersburg, Maryland 20899, United States

Supporting Information

**ABSTRACT:** In this work, we use constant load indentation and cantilever peel of polymer films to probe relaxation events that occur due to the chemical modification of a buried interface. Hydroxypropyl cellulose films on four different chemical interfaces were produced, and the creep compliance and fracture energy of each interface was measured. Polymer films having strong interfacial interactions with the substrate, as measured by cantilever peel, exhibited equivalent compliance to bulk measurements when modeled as a thin film with a perfectly bonded (no slip) interface. On weaker interfaces, larger contact areas led to this model calculating significantly higher compliances than expected, which we attribute to debonding events at the interface. These additional relaxations at the buried interface were strongly dependent on the extent the substrate surface moieties could hydrogen bond with the hydroxyl groups present on the polymer chain. Deviations caused by debonding events were additive over time, with modeled compliance up to 250% greater than bulk compliance. By modifying the polymer–substrate interface, the strength and durability of different chemical interactions at the interface can be studied and used to design robust interfacial interactions for improved performance.



## INTRODUCTION

Thin films and polymer coatings are widely applied to modify material properties for chemical, mechanical, or aesthetic reasons. Because of chemical or mechanical mismatches between the film and substrate, strong interfacial bonding and adhesive strength can be difficult to develop, and long-term stability is affected by interfacial stresses formed upon film formation or during use. Internal stresses within the coating can cause permanent deformation or even delamination over time as a result of viscoelastic or interfacial relaxations.<sup>1</sup> These effects are increasingly prevalent as novel materials are designed around high interfacial contact of dissimilar materials. Polymer–matrix nanocomposites and layer-by-layer films have significant fractions of the sample dominated by interfacial regions. Here, just as in a simple thin film, the adhesion, aging and stress response at interfaces will have a critical effect on overall performance.<sup>2–5</sup> Isolating the properties of these interfacial regions is difficult since interfacial contributions are mixed with bulk responses. The ability to decouple the material response of the interfacial regions from the bulk would greatly improve the prediction of lifetime performance and isolate key design parameters.

The most common interfacial measurements are derived from adhesion experiments, which typically involve calculating an adhesion parameter from the separation of a well-defined geometry under an applied load.<sup>6,7</sup> In peel experiments, the interfacial adhesion energy is determined from the applied force to propagate a crack, or peel front. This technique has been adapted to measure the adhesion of patterned surfaces, rate-dependent materials, or surface coatings within a controlled experimental

design.<sup>8,9</sup> An alternate method uses contact mechanics of a compliant indenter with a flat substrate, using models such as the Johnson, Kendall, Roberts (JKR) theory to quantify the work of adhesion between the two contacting surfaces through a loading and unloading cycle.<sup>10</sup> These experimental designs provide a planar surface, so the surface can be modified to measure a variety of materials, such as pressure sensitive adhesives, biological interfaces, and biomimetic surfaces.<sup>11–14</sup> To test for failure of an interface, a sufficient load can be applied by a rigid indenter to delaminate a buried interface, where the delamination stress and crack formation is controlled by the indenter geometry, the film thickness, and the strength of the buried interface at the point of failure.<sup>15,16</sup>

Before delamination occurs, the mechanical properties of a multilayered substrate can be inferred from contact mechanics models. Each layer contributes to the indentation response dependent on the thickness and modulus of each layer and the stress transfer between layers. An interface with strong adhesion and perfect shear stress transfer (pure bonded), and an interface with no adhesion or shear stress transfer (pure slip) would be considered the maximum and minimum level of shear stress which can be transferred at the interface, respectively.<sup>17–19</sup> In previous work, we have detected nonideal interfaces through constant load indentation of a multilayered substrate with a poorly adhered polymer–substrate interface.<sup>20</sup> These weak interfaces have properties between the ideal cases of pure bonded and pure slip conditions, with distinct relaxation mechanics

Received: February 25, 2011

Published: April 14, 2011

independent of the bulk polymer relaxations. When interfaces were poorly designed and the polymer was able to translate along the interface, the growth of the contact area increased as compared to a molecularly bonded interface.

In this work, we measure interfacial relaxations caused by variations in surface chemistry presented at the interface between a glass substrate and a hydroxypropyl cellulose coating. By controlling the hydrogen-bonding potential of the glass substrate, we systematically change the strength and number of hydrogen-bonding sites at the buried interface, which in turn affects the subsequent indentation profile. By varying the density of hydroxyl, carboxylic acid, alkyl, or fluorine groups on the glass substrate, the extent and rate of indentation contact area growth was correlated to the hydrogen-bonding potential at the polymer–substrate interface. If these measurements are used to calculate compliance as if the interface was purely bonded, then strongly adhered interfaces matched the bulk compliance while the compliance as measured on weakly adhered interfaces did not, effectively allowing for the deconvolution of the bulk and interfacial responses. Cantilever peel measurements on the same interfaces were performed to obtain the fracture energy and confirm the relaxations occurring at the buried interface are related to the interfacial adhesion strength.

## EXPERIMENTAL SECTION

**Materials.** Equipment, instruments, and materials are identified in the paper in order to adequately specify the experimental details. Such identification does not imply recommendation by the National Institute of Standards and Technology (NIST), nor does it imply the materials are necessarily the best available for the purpose. Hydroxypropyl cellulose (HPC) (mass average molecular mass of  $10 \times 10^5$  g/mol) was obtained from Sigma-Aldrich (Milwaukee, WI). Octyl dimethylchlorosilane and tridecafluoro-1,1,2,2-tetrahydrooctyl dimethylchlorosilane were obtained from Gelest (Morrisville, PA). Norland Optical Adhesive 81 was purchased from Norland Products (Cranbury, NJ). All chemicals were used as received.

**HPC-Glass Interface Preparation.** Glass substrates were treated with either chlorosilanes or ultraviolet/ozone (UVO) to create fluorinated, alkyl, carboxylic acid, or silanol (hydroxyl) groups at the surface. When coated with HPC, these surfaces present a continuous, homogeneous chemistry comprised of a single type of functional group to the polymer. Water contact angle measurements were performed using a Krüss DSA 100 drop shape analyzer (Nazareth, PA), and multiple spots were measured across each substrate to confirm uniformity of surface treatment.

Each substrate was prepared with two different interfaces, created by isolating the silane deposition or UVO treatment to one-half of the slide. Limiting the silane deposition to half the substrate is described in detail elsewhere.<sup>20</sup> To briefly summarize, glass slides were cleaned with toluene and ethanol, dried, and exposed to UVO for 500 s. Silane deposition was isolated on one-half of the glass substrate by immersing one-half of the slide and protecting the other half with a sacrificial glass superstrate. The glass superstrate was held in place by placing a small drop of water on the substrate prior to lamination. The exposed region was immersed in a toluene solution containing 10% by mass of the appropriate silane for 900 s, and water on the protected region prevented any silane deposition due to immiscibility of toluene with water. After silane deposition, slides were cleaned with toluene and water, dried, and then stored under vacuum

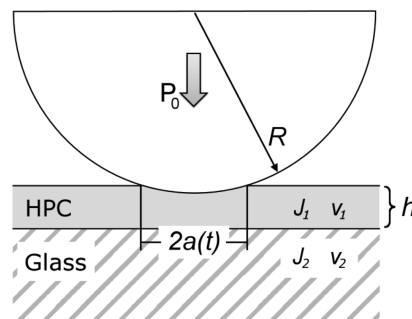


**Figure 1.** Thin film indentation geometry used for experimental modeling and design, using an indenter of radius,  $R$ , with a constant load,  $P_0$ , throughout the experiment. The contact radius,  $a(t)$ , depends on the top layer film thickness,  $h$ , the compliance,  $J$ , and Poisson's ratio,  $\nu$ , of each layer.

until used. The protected region was left unaltered, to provide a control region with a hydroxyl surface.

Two different silanes, octyl dimethylchlorosilane and tridecafluoro-1,1,2,2-tetrahydrooctyl dimethylchlorosilane, were deposited to form surfaces with alkyl and fluorinated groups, respectively. For the hydrogen-bonding surface, hydroxyl chemical moieties were created from the initial UVO treatment of the glass. A second hydrogen-bonding surface was formed by UVO irradiation of an alkyl silane monolayer. This has been shown to create carboxylic acid functional groups at the surface, and the extent of exposure controls the density of carboxylic acid groups.<sup>21</sup> By increasing the duration of UVO treatment, the surface coverage of carboxylic acid functional groups capable of hydrogen bonding increases. This treatment was varied systematically to create mixed interfaces which simultaneously contain both carboxylic acid and alkyl functional groups at the surface. Alkyl silane substrates were irradiated for three different exposure times: 40, 20, and 10 s, with the 40 s exposure time sample denoted as a carboxylic acid surface. Water contact angles were not significantly different on the protected half of the substrate, except for a 5 mm-wide region between the silane treated and protected half of the sample. Since changes in the average density of functional groups within the indentation area could affect the stress relaxation profile, the boundary region was ignored and no experiments were performed in this region.

HPC films were flow coated on glass substrates using a solution of anhydrous ethanol with 8.0% by mass HPC. Films were dried first in air for 4 h and then stored in vacuum for at least 24 h prior to experimentation. In addition, HPC films were produced on silicon wafers using the same flow coating parameters for film thickness measurements, which required a reflective surface. Film thickness was measured to be  $4.4 \mu\text{m} \pm 0.2 \mu\text{m}$  using a Filmetrics F20 spectral reflectometer (San Diego, CA). These measurements were corroborated with the measured film thickness of HPC films transferred to silicon from fluorinated or alkyl-modified glass substrates. Bulk films were prepared from repeated flow coating of more concentration HPC solutions, building  $\approx 0.5$  mm thick substrates.

**Thin Film Indentation.** Indentation of thin HPC polymer films was performed by monitoring the contact area of a fixed load spherical indenter over time. This technique was modified from a high-throughput bulk viscoelastic indentation technique, which used the gravity load of metal spheres to indent the polymer film<sup>20,22</sup> and is shown schematically in Figure 1. For

these experiments, the indenter size was increased to 12.7 mm diameter chrome steel spheres to produce larger contact areas and higher loads. At each contact area, optical images were taken over time and then analyzed to determine contact radii, which were then related to the polymer compliance. An indenter holder for four spheres was combined with a vertical motion stage to place all spheres on the surface simultaneously and allowed for multiple indentations to be measured on each sample. A Leica DMIRE2 inverted optical microscope (Wetzlar, Germany) imaged each contact area, sequentially traveling to each indentation position within the array.

After all images were collected, the indentation contact radii were determined with an image processing method using edge detection and Hough transforms to locate the contact area and radius. With larger radii indenters, small increases in the indentation depth translated into significant contact area growth, providing sufficient resolution to discriminate between small changes in compliance. Contact radii for these experiments ranged from 35 to 53  $\mu\text{m}$ , and indentation depths did not exceed 3% of the film thickness. Array indentation were performed for 10000 s to determine long time compliance effects, with a minimum of 20 s between images. To quantify short time effects, single sphere indentations were imaged for 120 s with 0.8 s between images to measure compliance at shorter time intervals. Both long and short time indentation experiments matched at equivalent indentation times. All experiments were performed at 22  $^{\circ}\text{C}$  in ambient air.

In this experimental design, the indentation of a purely bonded interface would be a combination of the compliance of the polymer film and the compliance of the glass substrate. Various models are available to determine the properties of a multilayered substrate, which vary dependent on the boundary conditions at the interface and the limitations of the models. The compliance measurements for this work were calculated from a model derived for a perfectly bonded interface. This model was described in work by Chen and Engel and was chosen because of the flexibility in material parameters and applicability over a wide range of  $a/h$  values.<sup>18,23</sup> The geometry used by Chen and Engel is equivalent to the design shown in Figure 1. The model iteratively solves for the compliance of the top layer using the contact radius of the multilayered substrate,  $a$ , measured during the experiment. For this solution, material properties for the glass substrate, the polymer film thickness, and an initial estimation for the compliance of the top layer are required to begin calculations and determine the compliance. A detailed explanation of the model and the computational solution is given in the Supporting Information.<sup>22</sup> Modeled compliance would only be equivalent to bulk compliance if the purely bonded interface assumption held.

In all experiments performed in this work, a constant film thickness was maintained to compare contact radii directly and to create a similar stress field at the interface for all indentations. Error bars for all indentation and water contact angle measurements in this paper is reported as 95% confidence intervals with at least four measurements, which provide an estimate of the standard uncertainty of the measurement. For indentation experiments, this error includes measurement error in the contact radii, which was detailed in previous work.<sup>22</sup>

**Cantilever Peel.** The fracture energy of the polymer–glass interface, which is analogous to adhesion, was measured by using mechanical relationships derived for peeling of a compliant slab from a rigid substrate.<sup>24</sup> Detailed descriptions of the experiment are presented elsewhere.<sup>25,26</sup> To briefly summarize, a glass

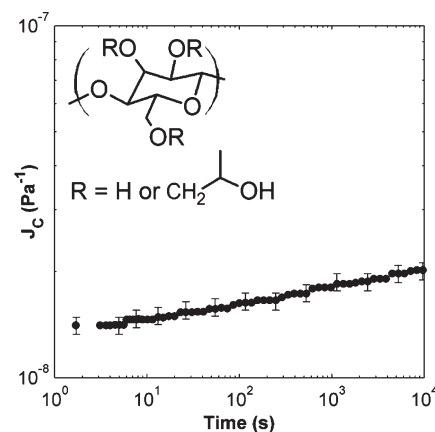


**Figure 2.** Hydroxypropyl cellulose (HPC) compliance measured on a 500  $\mu\text{m}$  thick polymer film. The chemical structure of HPC is shown in the inset, where either hydroxyl or hydroxypropyl units are attached to the cellulose ring. Indentations were performed on 100  $\mu\text{m}$  thick HPC films at 22  $^{\circ}\text{C}$ .

cantilever of known elastic properties was fixed to HPC film using Norland Optical Adhesive 81, a photocurable adhesive. A metal spacer attached to a load cell lifted the cantilever at a rate of 5  $\mu\text{m/s}$ , causing the cantilever-polymer to peel from the chemically modified substrate. The peel event was recorded optically and images were correlated with load–displacement data to determine fracture energy. Delamination occurs at the weakest interface, so this experimental technique can only measure fracture energy of that interface. The strength of the adhesive–HPC interface set the upper bound for the measurable fracture energy of the HPC–substrate interface, since a stronger HPC–substrate interface would cause delamination from the adhesive–HPC interface. The adhesive–HPC interface had a fracture energy of  $420 \text{ mJ/m}^2 \pm 16 \text{ mJ/m}^2$ ; thus, the test as implemented could characterize polymer–substrate interfaces weaker than this critical value. Cantilever peel measurements are presented with standard error at 95% confidence intervals, which provides an estimate of the standard uncertainty of the measurement. Fracture energy is then calculated from four independent measurements.

## RESULTS AND DISCUSSION

Before thin film indentation, a bulk HPC film was measured to determine time-dependent HPC compliance without interfacial effects. For these experiments, only Hertzian contact mechanics are needed to determine the compliance of the polymer network. The results from the bulk polymer film provided a baseline compliance value for HPC with a perfectly bonded interface. In the thin film indentation experiments, the compliance of HPC in the thin film is assumed to be equivalent to the bulk polymer network. The only difference is a manifestation of any interfacial effects that occur and will contribute to the indentation response. The compliance measured for a bulk HPC film is shown in Figure 2. In this case, the bulk film and smaller spheres (3.0 mm diameter) were used; these parameters limited the indentation measurement to bulk polymer relaxations. The compliance measured for bulk HPC films showed only a small amount of viscoelastic relaxation after an indentation of 10000 s. The compliance and viscoelastic behavior are similar to other measurements reported in literature.<sup>27</sup> Hydrogen bonding present in the

**Table 1. Surface and Interfacial Properties of Chemically Modified Substrates**

chemical structure	water contact angle (deg)	fracture energy (mJ/m <sup>2</sup> )
fluorinated	111 ± 4	0.21 ± 0.01
alkyl	97 ± 3	7.78 ± 0.27
carboxylic acid	23 ± 2	>420 ± 16
hydroxyl	<10	>420 ± 16

HPC chain provides an additional resistance to chain relaxations, which in turn reduces the change in compliance over time. Since internal hydrogen bonding is critical to the reduced creep exhibited in the bulk compliance, interfaces with the potential for hydrogen bonding should limit interfacial relaxations. The four substrate treatments, previously described, were prepared to test a broad range of surface interactions.

**Homogenous Interfaces.** To quantify the adhesion of the hydrogen-bonding and non-hydrogen-bonding substrates, cantilever peel measurements were performed. Fracture energy and water contact angle measurements are shown in Table 1. The hydrophilic surfaces, carboxylic acid and hydroxyl, delaminated at the adhesive-polymer interface and had a fracture energy exceeding the measurement capability. In contrast, the non-hydrogen bonded fluorinated and alkyl surfaces delaminated at the polymer-substrate interface. The fracture energy required was inversely correlated with water contact angle, with the highest water contact angle surface having the lowest fracture energy. Significant variations occurred from changes in surface chemistry, with an order of magnitude increase in fracture energy going from fluorinated to alkyl surfaces. To delaminate hydrophilic interfaces, at least another 2 orders of magnitude of fracture energy would be required as compared to hydrophobic interfaces. For peel experiments, the hydrogen-bonding groups at the interface facilitated a significant enhancement of the fracture energy required to irreversibly delaminate the interface.

With an understanding of the fracture energy of the polymer substrate interface, indentation contact radii were measured for films on the fluorinated, alkyl, carboxylic acid, and hydroxyl interfaces for 10000 s. The indentation contact radii and the previously described model were used to determine the compliance of each HPC indentation, and the results for each interface type are shown in Figure 3. The indentation model for determining polymer film compliance assumes a perfectly bonded interface, which clearly is not the case in the fluorinated or alkyl surfaces based on cantilever peel measurements.

In Figure 3, both interfaces with hydrogen-bonding moieties matched compliances from bulk measurements, while the alkyl and fluorinated interfaces displayed significantly higher modeled compliance. When present, polar groups on the glass substrate and within the hydroxypropyl cellulose chain developed significant hydrogen bonding at the interface. Since the model to quantify HPC compliance relies on a perfectly bonded interface, compliances matching the bulk polymer demonstrate the lack of interfacial relaxations. This purely bonded interface assumption is further supported by inability to delaminate these surfaces with cantilever peel. For the alkyl and fluorinated interfaces, the model-calculated compliance was higher than predicted, caused by the failure of the perfect bonding condition due to molecular debonding events at the polymer-substrate interface. The hydroxyl groups on the HPC chain cannot hydrogen bond with an interface presenting alkyl and fluorine moieties, resulting in

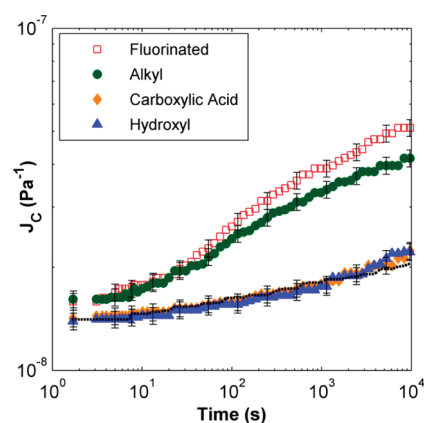


**Figure 3.** Creep compliance as deduced from a bonded model for four different glass substrate treatments and the bulk compliance (---). Compliance measured on hydrophilic interfaces match the bulk compliance results, while hydrophobic interfaces exhibit a higher than expected compliance due to an increase in contact radii, indicative of debonding events at the interface. All modeled compliance results were collected from indentations on 4.4  $\mu\text{m}$  thick HPC films at 22  $^{\circ}\text{C}$ .

weaker adhesion and eventual failure of the bonded interface assumption. The relative ranking of the surface treatments corroborates the cantilever peel experiments, with the fluorinated interface having the weakest fracture energy and greatest deviation from bulk compliance.

The apparent increase in compliance as compared to bulk measurements was not due to inherent changes of the viscoelastic properties of HPC, but from contributions not captured by a model based on a purely bonded interface. At short times, the lack of debonding events caused the indentations to appear similar to each other, but steadily separated as the cumulative effect of successive debonding events allowed polymer translation at the interface and a corresponding increase in the contact radii. The interfacial relaxations developed simultaneously with the polymer relaxations, and these interfacial effects alone contribute to the deviation in the modeled compliance. This change in the interfacial stress transfer resulted in significantly different contact radii for different surface chemistry. For example, the contact radius at 1800 s for the fluorinated interface indentation was  $49.5 \mu\text{m} \pm 0.4 \mu\text{m}$ , as compared to the hydroxyl interface contact radius of  $42.9 \mu\text{m} \pm 0.4 \mu\text{m}$ . Since the interfacial response requires time to develop sufficiently, similar interfaces such as the carboxylic acid and hydroxyl surfaces would likely require further indentation or elevated temperature to distinguish any differences between these two interfaces.

**Mixed Interfaces.** With the first set of experiments, the designed interfaces were prepared to present a single chemical moiety with large differences in water contact angle, fracture energy, and hydrogen-bonding potential. Since there was a significant difference between the alkyl and carboxylic acid interface measurements, mixed interfaces containing both chemical moieties were prepared to determine the effect of limited numbers of hydrogen-bonding groups at the surface. In addition to the homogeneous alkyl and carboxylic acid interfaces, two intermediate UVO treatments were performed on the alkyl silane monolayer to form a mixed surface containing both alkyl and carboxylic acid groups. HPC films were formed using the same conditions as previously stated. The compliance measurements for the four different interface types and the bulk measurement are shown in Figure 4.

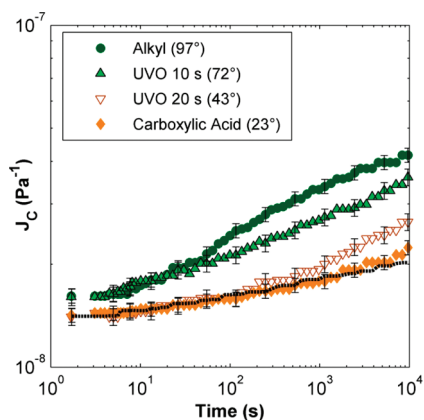


**Figure 4.** Compliance measurements for indentations of hydroxypropyl cellulose on an octyl (alkyl) silane substrate and three ultraviolet ozonolysis (UVO) treated alkyl silane substrates, along with the measured bulk compliance (---). Water contact angles for all four systems are given, with a decrease in contact area growth with decreasing hydrophobicity. All interface compliance measurements were indentations on 4.4  $\mu\text{m}$  thick HPC films at 22  $^{\circ}\text{C}$ .

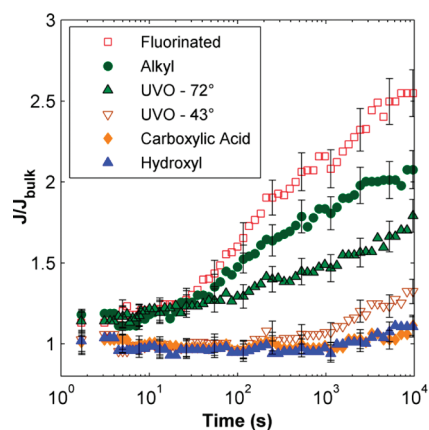


**Figure 5.** Normalized compliance, using the bulk HPC compliance measurements and bonded model compliance for all developed interfaces. The two hydrogen-bonded interfaces show minimal deviation, while the weaker interfaces deviate dramatically from the reduced compliance at different rates.

All four systems separated into two response types dependent on the interface being more hydrophilic or more hydrophobic. The modeled compliance for each system was significantly different at 10000 s, and the two mixed interfaces had modeled compliance between the two chemically homogeneous interfaces. With an increase in the density of carboxylic acid groups at the surface, the polymer chains had more opportunities to adhere strongly by forming hydrogen bonds at the interface. Hydrogen bonding at the interface reduced the amount and extent of debonding events at the surface, resulting in less deviation from bulk compliance. In particular, the separation of the more hydrophilic mixed interface required (CR) 2500 s to appear significantly different from the bulk compliance. At shorter times, the modeled compliance appears equivalent, since a low number of debonding events required more time to accumulate into a detectable deviation from a purely bonded interface.

One problem with measuring compliance of the polymer film on weak interfaces is that the intrinsic polymer relaxations leading

to the increase in bulk compliance have not changed, only the interfacial effects. Isolating the interfacial response and decoupling the bulk compliance would allow for an improved representation of the interfacial response to be analyzed. To remove the effect of the bulk viscoelastic relaxations, modeled compliance from all experiments were normalized to the bulk viscoelastic compliance. The normalized compliance,  $J/J_{bulk}$  is shown for all six interfaces in Figure 5. The normalized compliance should equal unity when the interface is perfectly bonded throughout the experiment, while a system with debonding events at the interface will have a normalized compliance above unity. For the systems shown here, only the hydroxyl and carboxylic acid surfaces have interfaces that match the bulk compliance over the time scale of the entire experiment. For the other prepared interfaces, the normalized compliance increases over time, with the weakest interface showing the greatest increase in the normalized compliance. The normalized compliance steadily increases as the experiment proceeds, since the deviations caused by debonding events can only further increase the contact area. In particular, more hydrophilic interfaces reduced the rate at which the normalized compliance deviated from unity, with the two most hydrophilic interfaces having sufficient strength to act as a perfect bonded interface throughout the indentation.

## CONCLUSIONS

With constant load indentations of thin polymer films, we were able to measure indentation responses that deviated from bulk polymer behavior due to changes in adhesion at a buried interface. In cases where the interface had limited hydrogen-bonding potential, interfacial relaxations made the perfectly bonded interface assumption invalid. This failure increased the contact area and caused the as-modeled polymer compliance to appear higher than expected. For interfaces with the potential for hydrogen bonding at the surface, the bonded interface assumption remained valid and the as-modeled polymer compliance was equivalent to the bulk compliance. The fracture energy as seen from cantilever peel measurements strongly correlated with the extent of interfacial relaxations, and both were able to discriminate between the interfacial strength created by different chemical moieties at the interface.

Interfacial relaxations could also be enhanced by reducing the density of hydrogen-bonding groups, which decreased the number of available locations for polymer chains to adhere strongly at the interface. The ability to probe nondestructively probe interfacial relaxations could be particularly informative when assessing the interfacial contribution in nanocomposites or multilayer polymeric structures where individual buried interfaces are not easily accessible. Though these effects require significant time to develop, the interfacial relaxations provide insight into the overall effect of interfacial failures in applications where a continual stress is applied. Since both the short-term and long-term effects of an interface contribute to the polymer application longevity, the ability to detect or locate suboptimal interfacial bonding prior to complete failure permits lifetime monitoring of polymer films and can greatly facilitate optimization of material interfaces.

## ASSOCIATED CONTENT

**S Supporting Information.** Description of heterogeneous indentation model, MATLAB methodology, and HPC example

indentation measurements. This material is available free of charge via the Internet at <http://pubs.acs.org>.

## AUTHOR INFORMATION

### Corresponding Author

\*E-mail: [chris.stafford@nist.gov](mailto:chris.stafford@nist.gov).

## ACKNOWLEDGMENT

P.M.J. and J.A.H. would like to thank the National Institute of Standards and Technology/National Research Council Postdoctoral Fellowship Program for funding.

## REFERENCES

- (1) Feng, C. W.; Keong, C. W.; Hsueh, Y. P.; Wang, Y. Y.; Sue, H. J. *Int. J. Adhes. Adhes.* **2005**, *25* (5), 427–436.
- (2) Dean, G. *Int. J. Adhes. Adhes.* **2007**, *27* (8), 636–646.
- (3) Bucknall, D. G. *Prog. Mater. Sci.* **2004**, *49* (5), 713–786.
- (4) Ghatak, A.; Vorvolakos, K.; She, H. Q.; Malotky, D. L.; Chaudhury, M. K. *J. Phys. Chem. B* **2000**, *104* (17), 4018–4030.
- (5) Song, R.; Chiang, M. Y. M.; Crosby, A. J.; Karim, A.; Amis, E. J.; Eidelman, N. *Polymer* **2005**, *46* (5), 1643–1652.
- (6) Kinloch, A. J., *Adhesion and adhesives: science and technology*. Chapman and Hall: London, 1987.
- (7) Johnson, K. L., *Contact Mechanics*. Cambridge University Press: New York, 1987.
- (8) Hamade, R. F.; Dillard, D. A. *Int. J. Adhes. Adhes.* **2005**, *25* (2), 147–163.
- (9) Lai, Y. H.; Dillard, D. A. *J. Adhes.* **1996**, *56* (1–4), 59–78.
- (10) Shull, K. R. *Mater. Sci. Eng., R* **2002**, *36* (1), 1–45.
- (11) Olesiak, S. E.; Oyen, M. L.; Ferguson, V. L. *Mech. Time-Depend. Mater.* **2010**, *14* (2), 111–124.
- (12) Nolte, A. J.; Chung, J. Y.; Walker, M. L.; Stafford, C. M. *ACS Appl. Mater. Interfaces* **2009**, *1* (2), 373–380.
- (13) Paiva, A.; Sheller, N.; Foster, M. D.; Crosby, A. J.; Shull, K. R. *Macromolecules* **2000**, *33* (5), 1878–1881.
- (14) Shull, K. R.; Crosby, A. J. *J. Eng. Mater. Technol.* **1997**, *119* (3), 211–215.
- (15) Ritter, J. E.; Lardner, T. J.; Rosenfeld, L.; Lin, M. R. *J. Appl. Phys.* **1989**, *66* (8), 3626–3634.
- (16) Vasinonta, A.; Beuth, J. L. *Eng. Fract. Mech.* **2001**, *68* (7), 843–860.
- (17) Chadwick, R. S. *SIAM J. Appl. Math.* **2002**, *62* (5), 1520–1530.
- (18) Chen, W. T.; Engel, P. A. *Int. J. Solids Struct.* **1972**, *8* (11), 1257–1281.
- (19) Jaffar, M. J. *J. Mech. Phys. Solids* **1988**, *36* (4), 401–416.
- (20) Johnson, P. M.; Stafford, C. M. *ACS Appl. Mater. Interfaces* **2010**, *2* (7), 2108–2115.
- (21) Roberson, S. V.; Fahey, A. J.; Sehgal, A.; Karim, A. *Appl. Surf. Sci.* **2002**, *200* (1–4), 150–164.
- (22) Johnson, P. M.; Stafford, C. M. *Rev. Sci. Instrum.* **2009**, *80* (10), 103904.
- (23) Chen, W. T. *Int. J. Eng. Sci. (Oxford, U. K.)* **1971**, *9* (9), 775–800.
- (24) Kendall, K. *Proc. R. Soc. London, A* **1975**, *341* (1627), 409–428.
- (25) Ghatak, A.; Mahadevan, L.; Chung, J. Y.; Chaudhury, M. K.; Shenoy, V. *Proc. R. Soc. London, A* **2004**, *460* (2049), 2725–2735.
- (26) Ghatak, A.; Mahadevan, L.; Chaudhury, M. K. *Langmuir* **2005**, *21* (4), 1277–1281.
- (27) Moe, D. V.; Rippie, E. G. *J. Pharm. Sci.* **1997**, *86* (1), 26–32.